[5] N. SAITO, K. HIRANO, K. OKUYAMA, and I. OKADA, Z. Naturforsch. **27 a**, 288 [1972].
[6] S. WUHL, F. LANTELME, and M. CHEMLA, J. Chim. Phys. **65**, 488 [1968].
[7] F. LANTELME and P. TURQ, J. Inorg. Nucl. Chem. **33**, 4025 [1971].
[8] A. LUNDÉN, Z. Naturforsch. **21 a**, 1510 [1966].
[9] H. KANNO, J. Nucl. Sci. Technology **7**, 428 [1970].
[10] I. OKADA, Thesis, Tokyo 1966.
[11] J. E. FREUND, Mathematic. Statistics, Prentice-Hall, Englewood Cliffs, N. J. 1962.
[12] It is quite likely that we underestimated the temperature in the separation tube somewhat for our old experiments with pure rubidium nitrate [8], but that we overestimated it in the case of a $LiNO_3-RbNO_3$ mixture [13]. Furnace temperatures are quoted in Table 1 for Okada's experiments.
[13] A. LUNDÉN, Ann. N.Y. Acad. Sci. **79**, 988 [1960].
[14] A. LUNDÉN and A. EKHED, unpublished.
[15] A. LUNDÉN, submitted to J. Inorg. Nucl. Chem.
[16] For run 1 and 4 there is a considerable spread in the obtained values of the mass effect. If we exclude the highest value for these two runs, we obtain an equation for μ_{Rb} with practically the same temperature coefficient as in Eq. (1) but wtih a 5% lower absolute value at 350 °C.
[17] I. OKADA and A. LUNDÉN, work in progress.

Transport Properties of Thoria and Thoria-based Solid Solutions

T. H. ETSELL

Max-Planck-Institut für Chemie (Otto-Hahn-Institut), Mainz

(Z. Naturforsch. **27 a**, 1138—1149 [1972]; received 24 March 1972)

The methods for obtaining transport numbers in oxides are described and associated experimental difficulties are discussed. Their reliability is assessed and used in conjunction with related data to offer a consistent picture for thoria and thoria-based solutions between 500° and 1600 °C. Both are ionic conductors within certain ranges of oxygen pressure. It is concluded that, for ThO_2,

$$\log P_{\oplus} = -4.5\,, \qquad \log P_{\ominus} \sim -\frac{60.5\times10^3}{T} + 23.3$$

and, for $ThO_2-Y_2O_3$ solutions (10—20 mole % $YO_{1.5}$),

$$\log P_{\oplus} = 1.8\,, \qquad \log P_{\ominus} = -\frac{57.9\times10^3}{T} + 12.4$$

where $P_{\oplus}$ and $P_{\ominus}$, respectively, are the oxygen pressures (atm) where the ionic and p-type and the ionic and n-type conductivities are equal. Ionic conductivity and charge carrier mobilities in thoria are briefly considered.

Transport properties of refractory oxides are important in the oxidation of metals, sintering, solid state reactions, and in their ceramic, electronic, nuclear, and aerospace applications. In the case of ThO_2-based solid solutions (containing CaO, Y_2O_3, or a rare earth oxide), they are of further importance since these systems by virtue of a high concentration of oxygen vacancies behave as oxygen-ion conducting solid electrolytes over certain ranges of temperature and oxygen pressure. Although their low ionic conductivities and p-type conductivity at high oxygen pressures preclude their use in batteries or fuel cells, they have found wide application in emf measurements to determine thermodynamic properties, particularly of systems exerting low oxygen potentials [1].

Nevertheless, as difficult high-temperature measurements are involved, the available data on their transport properties, particularly at low oxygen pressures, are widely scattered. Recently, an analysis was presented for stabilized zirconia electrolytes [2] in an effort to account for some of the discrepancies existing in their case. Herein, a similar analysis is made for thoria-based solutions. Results for thoria are included for comparison. The emphasis will be on transport numbers since they are of major importance in solid electrolyte applications.

The different experimental techniques available to determine transport numbers in oxides will be briefly reviewed and later discussed and assessed for reliability. From this assessment and related emf data, the best estimate of the transport numbers for thoria and thoria-based solutions will be offered.

Reprint requests to Dr. T. H. ETSELL, Department of Metallurgy and Materials Science, University of Toronto, *Toronto 5*, Ontario, Canada.

Methods of Determining Transport Numbers in Oxides

The most direct method involves measuring the a – c conductivity as a function of oxygen pressure

and subsequently analyzing the curves to separate the ionic and electronic contributions. Behaviour of the partial conductivities of oxides exhibiting significant ionic conduction is typified by that of ThO_2 + 14 mole % $YO_{1.5}$ evident in Fig. 1 (based on the present analysis). P-type and n-type conductivity arise from a stoichiometric excess and deficit of oxygen in the lattice, respectively. Ionic and p-type conductivity invariably show a much weaker temperature dependence than n-type conductivity causing $P_\ominus$ and the p-n transition to shift rapidly to higher oxygen pressures with increasing temperature. Ionic conductivity to be significant implies a high lattice defect concentration and is, therefore, almost always independent of oxygen pressure. Then, excluding the possibility of impurity-controlled electronic conduction (impurities and electronic defects dominate the neutrality condition) or intrinsic electronic conduction (unlikely below 1600 °C), a region where the total conductivity is oxygen pressure-independent represents ionic conductivity. As the ionic transport number, t_i, is defined as $t_i = \sigma_i/(\sigma_i + \sigma_p + \sigma_n)$ where σ_i, σ_p, and σ_n are the ionic, p-type, and n-type conductivities, respectively, it can be readily calculated at any required oxygen pressure.

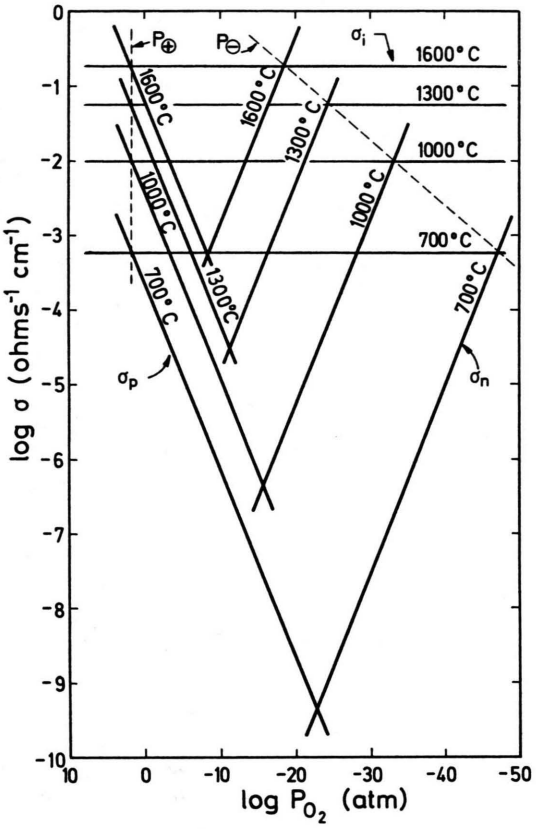

Fig. 1. Partial conductivities for ThO_2+14 mole % $YO_{1.5}$ ($Th_{0.86}Y_{0.14}O_{1.93}$).

In the absence of an oxygen pressure-independent region, since the total conductivity, σ_t, in a zone where either σ_p or σ_n is negligible can be written as

$$\sigma_t = \sigma_i + K P_{O_2}^{\pm 1/n} \qquad (1)$$

where K is a constant and the oxygen pressure exponent is positive for p-type and negative for n-type conduction, the ionic contribution can be determined by plotting σ_t against $P_{O_2}^{\pm 1/n}$ for possible values of n. The correct value of n will give a linear plot which is then extrapolated to $P_{O_2} = 0$. In all cases, it is preferable to check the validity of the assumption that oxygen pressure-independent conductivity is ionic conductivity with emf measurements.

The d-c polarization technique can also be used. For predominantly anionic conductors, a cathode which prohibits ionic current by not supplying oxygen to the sample is strongly polarized. The resulting electronic current, which is measured at several applied voltages, can then be related to the p- and n-type conductivities at the oxygen pressure imposed by the reversible anode.

The most common methods involve emf measurements. After SCHMALZRIED [3], for an oxide with measurable oxygen pressure-independent ionic conductivity and, therefore, low concentrations of electronic defects (small deviations from stoichiometry),

$$E_m = \frac{RT}{F}\left[\ln\frac{P_\oplus^{1/n} + P_{O_2}'^{1/n}}{P_\oplus^{1/n} + P_{O_2}''^{1/n}} + \ln\frac{P_\ominus^{1/n} + P_{O_2}''^{1/n}}{P_\ominus^{1/n} + P_{O_2}'^{1/n}}\right] \qquad (2)$$

where E_m is the measured emf, P'_{O_2} and P''_{O_2} are the oxygen pressures at the anode and cathode, respectively ($P''_{O_2} > P'_{O_2}$), and $P_\oplus$ and $P_\ominus$ are the oxygen pressures at which $\sigma_i = \sigma_p$ and $\sigma_i = \sigma_n$, respectively, i. e., $t_i = 0.5$. If the ionic defects are fully ionized (generally the case at high temperatures), $n = 4$. The thermodynamic emf, E_t, given by

$$E_t = (RT/4F)\ln(P''_{O_2}/P'_{O_2}) \qquad (3)$$

can be realized when $P_\oplus \gg P''_{O_2} > P'_{O_2} \gg P_\ominus$, i. e., $t_i = 1$.

Since the ionic transport number can be expressed as

$$t_i = \left[1 + \left(\frac{P_{O_2}}{P_\oplus}\right)^{1/4} + \left(\frac{P_{O_2}}{P_\ominus}\right)^{-1/4}\right]^{-1} \qquad (4)$$

knowledge of $P_{\oplus}$ and $P_{\ominus}$ is sufficient to calculate it at any given oxygen pressure. Invariably, either $P_{\oplus}$ or $P_{\ominus}$ is eliminated from Eq. (2) by a suitable choice of P'_{O_2} and P''_{O_2}. For example, regarding $P_{\oplus}$, if $P'_{O_2} \gg P_{\ominus}$,

$$E_m = \frac{RT}{F} \ln \frac{P_{\oplus}^{-1/4} + P'^{-1/4}_{O_2}}{P_{\oplus}^{-1/4} + P''^{-1/4}_{O_2}} \quad (5)$$

and for the condition $P_{\oplus} \gg P'_{O_2} \gg P_{\ominus}$, inspection of Eq. (2) and (4) leads to

$$E_m - E_t = \frac{RT}{F} \ln (t_i)_{P''_{O_2}} . \quad (6)$$

For the determination of $P_{\ominus}$, simplification of Eq. (2) can be similarly achieved [2]. Results are often reported via an average ionic transport number, $\bar{t}_i$, defined as

$$\bar{t}_i = E_m/E_t \quad (7)$$

from which $P_{\oplus}$ or $P_{\ominus}$ can be evaluated using Eq. (3), (7), and either (2), (5), or (6). This method, effectively dependent upon a comparison of E_m and E_t, will be referred to as the emf comparison technique.

Alternatively, $P_{\ominus}$ can be determined with a cell such that $P_{\oplus} \gg P''_{O_2} \gg P_{\ominus} \gg P'_{O_2}$ which yields a maximum emf, E_{max}, given by

$$E_{max} = (RT/4F) \ln (P''_{O_2}/P_{\ominus}) . \quad (8)$$

This method will simply be referred to as the maximum emf technique if the required low value of P'_{O_2} is established thermodynamically. If it is established electrochemically by temporarily applying a voltage to remove oxygen from the anode chamber, the method is usually called the coulometric titration technique although quantitative measurement of the coulombs passed is unnecessary. The applied voltage is progressively increased with emf measurements being taken subsequent to each step. The potentiometrically-detected end point appears when the cell emf ceases to depend on the applied voltage.

Additional methods are Faraday law experiments which involve passage of a known quantity of electricity through an oxide sample held between reversible electrodes (individual ionic contributions can be separated if two or more samples in series are used, i. e., Hittorf-type experiments), oxygen permeability measurements whereby the conductivity of the predominant charge carrier with the opposite charge of the species which has the highest conductivity is determined, and, finally, diffusion coefficient measurements in combination with the Nernst-Einstein relation and total conductivity data.

Thoria

Early studies by DANFORTH and co-workers [4–6] and later by PAL'GUEV and NEUIMIN [7] and STEELE and ALCOCK [8] indicated that ionic conductivity is quite significant in ThO_2 at intermediate oxygen pressures. More recently, LASKER and RAPP [9] showed conclusively that ThO_2 is virtually a pure ionic conductor under this condition.

Available $P_{\oplus}$ data for ThO_2 at 1000 °C are listed in Table 1. All samples were polycrystalline in the shape of disks, bars, or cylinders and were usually sintered between 1800° and 2200 °C. Values from the a – c conductivity studies were calculated by determining t_i at $P_{O_2} = 1$ or 10^{-2} atm and using Eq. (4) with $P_{O_2} \gg P_{\ominus}$. Use of Eq. (4) is justified because the required proportionality between σ_p and $P_{O_2}^{1/4}$ has been shown, using RUDOLPH's results [14], to be obeyed [9, 15] and has been confirmed [9, 11–13].

In the range 800° – 1200 °C, both a slight increase [9, 10] and decrease [12, 13] of the ionic transport

Table 1. Log $P_{\oplus}$ values for ThO_2.

Purity	Technique	Temperature Range [°C]	log $P_{\oplus}$ [atm] 1000 °C	Ref.
> 99.92	Emf comparison, air vs. O_2	1000–1400	– 5.5	10
99.82	A-c conductivity as function of P_{O_2}	800–1100	– 4.6	9
> 99.92	A-c conductivity as function of P_{O_2}	1000	– 5.5[a]	11
> 99.99	A-c conductivity as function of P_{O_2}	1000–1600	– 4.0	12
99.99	A-c conductivity as function of P_{O_2}	1000–1500	– 1.5	13

[a] For specimen III in this paper.

* This agreement may be somewhat fortuitous since ionic conductivities vary by an order of magnitude.

number with temperature have been indicated. Based on this fact and the good agreement in Table 1 * (excluding one value [13]), the best estimate of $P_{\oplus}$ is

$$\log P_{\oplus} = -4.5\ (800^{\circ} - 1200\ ^{\circ}\mathrm{C}). \qquad (9)$$

The apparent activation enthalpies for p-type and ionic conduction, respectively, are $\Delta H_p = 1.0$ eV [12, 13, 15] and $\Delta H_i \sim 1.0$ eV [6, 10, 12].

As yet, nothing definite can be said about higher temperatures except that any change in $P_{\oplus}$ will be slight. Recent work [12, 13] indicates that ΔH_p decreases to 0.8 eV at about 1200 °C meaning that $P_{\oplus}$ increases somewhat with increasing temperature and appears to be about 10^{-3} atm at 1600 °C based on an extrapolation of a low-temperature Arrhenius plot for σ_i [12]. However, the course of ΔH_i is uncertain and difficult to determine due to interference from σ_n [12, 13].

An estimation of $P_{\ominus}$ can be made as follows. Equating the expressions for n-type and ionic conductivity gives

$$\log P_{\ominus} = -1.7372\,(\Delta H_n - \Delta H_i)/RT + 4\log(A_n/A_i) \qquad (10)$$

where ΔH_n and ΔH_i are the apparent activation enthalpies for n-type and ionic conduction, respectively, and A_n and A_i are the pre-exponential terms which are generally not a significant function of temperature [2]. From uv absorption spectra [16, 17], the band gap in ThO_2 is about 5.0 eV. Since the sum of the defect reactions describing the formation of electron holes and excess electrons is the reaction for intrinsic electronic defect formation, $\Delta H_p + \Delta H_n \sim 5.0$ eV assuming holes and electrons are not appreciably trapped. Hence, $\Delta H_n \sim 4.0$ eV. From BRANSKY and TALLAN'S results [12], as the p-n transition occurs at 10^{-6} atm and $P_{\oplus} \sim 10^{-3}$ atm at 1600 °C, $P_{\ominus} \sim 10^{-9}$ atm at 1600 °C. Combining this point, $\Delta H_n = 4.0$ eV, and $\Delta H_i = 1.0$ eV with Eq. (10) yields

$$\log P_{\ominus} \sim -\frac{60.5 \times 10^3}{T} + 23.3\ (1000^{\circ} - 1600\ ^{\circ}\mathrm{C}). \qquad (11)$$

This equation is in reasonable agreement with recent conductivity data at 1300° – 1500 °C [13]. The low temperature limit is based on the qualitative agreement of Eq. (11) ($P_{\ominus} = 10^{-24}$ atm at 1000 °C) with the fact that, even with relatively insensitive conductivity measurements, LASKER and RAPP [9] observed an n-type contribution at 10^{-22} atm and 1000 °C. Nevertheless, based on the reported levels of aliovalent cation impurities thought indirectly responsible for ionic conduction (see below), somewhat higher $P_{\ominus}$ values for ThO_2 would be predicted using electrical property results for $ThO_2 - Y_2O_3$ solutions and a dilute solution theory [9].

Regarding ionic conduction in ThO_2, from self-diffusion coefficient measurements which indicate that $D_{O^{--}}$ [18] and $D_{Th^{4+}}$ [19] are about 10^{-7} and 10^{-14} cm²/sec at 1600 °C, respectively, the anions migrate about 10^7 times faster. Ionic conductivity data can be used to estimate $D_{O^{--}}$. Because $\sigma_i = 3.3 \times 10^{-5}$ Ω^{-1} cm^{-1} at 1000 °C [9] and $\Delta H_i \sim 1.0$ eV, $\sigma_i \sim 6 \times 10^{-4}$ Ω^{-1} cm^{-1} at 1600 °C. Combining this value with $[O^{--}]$ in ThO_2 (4.56×10^{22}/cm³) and the Nernst-Einstein equation results in $D_{O^{--}} = 3 \times 10^{-9}$ cm²/sec at 1600 °C. Although this is 1 – 2 orders of magnitude lower than that given above, recent $D_{Th^{4+}}$ data [20] are about two orders lower than the earlier results [19] supporting the factor of 10^7. The factor will be even greater at lower temperatures as the activation energies for O^{--} and Th^{4+} migration are 1.0 eV [6, 10, 12] and 2.5 eV [19], respectively. Clearly, cationic conductivity will be negligible.

It is interesting to note that ThO_2 along with La_2O_3 [21] and perhaps Sc_2O_3, Y_2O_3, and some of the rare earth oxides with stable trivalent cations [1] are the only nominally pure oxides which exhibit exclusively anionic conduction ($t_{O^{--}} > 0.99$) within certain ranges of temperature and oxygen pressure (low temperatures and intermediate oxygen pressures). For all these oxides, the anionic defects responsible for ionic conduction appear to be extrinsic in origin (their presence is due to impurities). The most probable lattice defects in ThO_2 are anion vacancies necessitated by substitutional di- and trivalent impurity cations (oxygen interstitials compensating either small interstitial or substitutional pentavalent impurity cations are also possible). More research is required in this regard. Surprisingly, higher ionic conductivities have been reported in the studies involving purer ThO_2 [12, 13]. However, it is noteworthy that, for very pure ThO_{2-x} (>99.99%), $x \propto P_{O_2}^{-1/6}$ from 10^{-2} to 10^{-6} atm and 1700° – 1900 °C [22] – the theoretical behaviour when doubly-ionized oxygen vacancies are the predominant lattice defect and their intrinsic and impurity-controlled concentration is negligible with

respect to that resulting from nonstoichiometry ($t_i \sim 0$).

Average impurity levels have been equivalent to about 0.04 mole % divalent cation impurities (0.02% anion vacancies). As conductivity can be expressed as

$$\sigma_k = c_k \mid z_k \mid e\, u_k \qquad (12)$$

where c_k, z_k, and u_k are the concentration, effective valence, and mobility of the migrating defect k, respectively, and e is the absolute value of the electronic charge, the oxygen vacancy mobility in ThO_2 can be estimated to be 1×10^{-5} cm²/V-sec at 1000 °C.

As expected, electronic defect mobilities appear to be higher. From thermoelectric power (Seebeck coefficient) results, BRANSKY and TALLAN [12] placed the lower limit of the hole mobility at about 6 cm²/V-sec at 1000 °C. This estimate is based on the assumption of small polaron hopping or narrow band semiconduction but seems rather high for this to be the case. It is in serious disagreement with a recently reported value of 10^{-5} cm²/V-sec at 1000 °C for the hole mobility in closely-related stabilized zirconia [23]. Concerning the excess electron mobility, x in ThO_{2-x} is 0.009 at 1600 °C and 10^{-10} atm of oxygen [22]. Under these conditions, $\sigma_n \sim 5 \times 10^{-3}\ \Omega^{-1}\,cm^{-1}$ (l. c. [12]). If each oxygen vacancy results in two excess electrons and the mobility of electrons is independent of their concentration, Equation (12) gives $u_n \sim 10^{-4}$ cm²/V-sec at 1600 °C. This is certainly a minimum estimate since x appears rather high when compared with the Th – O phase diagram [24]. Results showing $u_p > u_n$ are consistent with evidence that ThO_2 is exactly stoichiometric [22] at higher oxygen pressures than those where the p-n transition occurs [12, 13].

Lastly, regarding thermal transport in ThO_2, the ionic Seebeck coefficient is about 0.5 mV/°C at 1 atm oxygen and 1000° – 1200 °C and the transport entropy of oxygen interstitials, assumed to be the predominant lattice defect, is 14.5 cal/mole-°K over a wide range of oxygen pressures [12].

Thoria-based Solutions

Although virtually all the investigations of transport numbers in ThO_2-based solutions have dealt with $ThO_2 - Y_2O_3$, only small changes are expected upon varying the minor component [1]. Transport numbers are not a significant function of composition between 10 and 20 mole % $YO_{1.5}$ (2.5 – 5% anion vacancies) [9].

High Oxygen Pressures

The marked increase in ionic transport numbers that can be achieved by dissolving di- or trivalent metal oxides in ThO_2 to introduce a large fraction of anion vacancies (1 – 7%) is apparent for high oxygen pressures in Table 2. Conductivity data at $P_{O_2} = 1$ atm were treated identically as for ThO_2. The expected proportionality between σ_p and $P_{O_2}^{1/4}$ (in the absence of excessive hole trapping and ex-

Table 2. Log $P_\oplus$ values for ThO_2-based electrolytes.

Addition to ThO_2 [mole %]	Sample Shape	Purity	Technique	Temperature Range [°C]	log $P_\oplus$ [atm] 1000 °C	log $P_\oplus$ [atm] 1600 °C	Ref.
15% CaO	disk		Emf comparison, Ar-air vs. air	600–1000	2.5		7
5% $YO_{1.5}$	disk	> 99.91	Emf comparison, air vs. O_2	1000–1400	0.6		10
15% $YO_{1.5}$	disk	99.83	A-c conductivity as function of P_{O_2}	800–1100	1.4		9
10% $YO_{1.5}$	bar	> 99.91	A-c conductivity as function of P_{O_2}	1000	1.9		11
13% $YO_{1.5}$	disk	99.998	A-c conductivity as function of P_{O_2}	850–1600	1.1[a]	1.1[a]	25
15% $YO_{1.5}$	disk	99.82	D-c polarization, Au vs. Cu_2O-CuO	800 – 1000	3.5		26
15% $YO_{1.5}$	tube		Emf comparison, Mn-MnO vs. air	1500		1.6[b]	27
20% $YO_{1.5}$	tube		Emf comparison, H_2-H_2O vs. Ar-O_2	400 – 1000	1.8		28
29% $YO_{1.5}$	tube		Emf comparison, Pb-PbO vs. air	500– 700	2.0[c]		29
15% $YO_{1.5}$	disk		A-c conductivity as function of P_{O_2}	800–1000	2.0[d]		39
18% $YO_{1.5}$	tube		D-c polarization, N_2 vs. air	900–1100	–1.4		31

[a] Emf data were also obtained which gave similar results. [b] 1500 °C.
[c] Extrapolated from 700 °C. [d] Estimated.

* Some oxygen transfer is inevitable when the electronic transport number is finite. It causes low emf readings when high enough to polarize one or both electrodes.

cessive vacancy complexing or association) has been verified [9, 11, 28]. The $P_{\oplus}$ values from the emf comparison studies were taken directly [27, 29] or calculated from Eq. (5) [7, 10] or (6) [28]. Equation (4) rather than (5) can be used when the difference between the oxygen chemical potentials at the electrodes is small $[\log(P''_{O_2}/P'_{O_2}) \leqq 4]$ by assuming that $\bar{t}_i = t_i$ at $\bar{P}_{O_2}$ where $\log \bar{P}_{O_2} = (\log P''_{O_2} + \log P'_{O_2})/2$. The approximation improves as $\bar{t}_i \to 0.5$ and is exact when $\bar{t}_i = 0.5$.

Despite the experimental difficulties associated with a – c conductivity measurements on sintered polycrystalline samples such as proper homogenization and equilibrium during preparation [1], and elimination of the influence of gross imperfections [1] and frequency dispersion [32], especially at low temperatures, Table 1 has already provided evidence that this technique appears generally reliable at high oxygen pressures. Nevertheless, such measurements are insensitive to small changes [29] and data from regions where $t_i \sim 1$ should not be used to calculate $P_{\ominus}$ (or $P_{\ominus}$).

When $\log(P''_{O_2}/P'_{O_2})$ is small or $\bar{t}_i \sim 1$, the emf comparison technique can provide accurate data since oxygen transfer across the electrolyte will be low * providing, when gas mixtures are used, suitable separation of the electrode compartments can be realized.

The d – c polarization technique has already been indicated as generally unreliable for predominantly ionic conductors [2]. Small ionic currents arising from insufficiently blocked electrodes, surface and gas phase conduction, and the uncertain influence of the large potential drop at the cathode-electrolyte interface render accurate direct determinations of small electronic conductivities at high temperatures extremely difficult.

Among the a – c conductivity and emf results, the agreement in Table 2 is very good and serves to show that transport numbers are not greatly affected by vacancy concentration (% CaO/2 or % $YO_{1.5}$/4) in the range of 2.5 to 7% (the low value [10] is consistent with the low % $YO_{1.5}$). However, the temperature dependence of $P_{\oplus}$ is controversial having been shown to increase with temperature [7, 10, 28, 29], decrease with temperature [26, 31], and be essentially independent of temperature [9, 25]. As most of the data indicating an increase with temperature are derived from emf measurements at low temperatures (400° to 800 °C) where electrode polarization, which would cause low results, is quite probable and the d – c polarization technique is unpredictable, $P_{\oplus}$ for ThO_2-based electrolytes is best represented as temperature independent from 500° – 1600 °C. Based on the excellent agreement among five investigations [9, 11, 27–29],

$$\log P_{\oplus} = 1.8 \quad (500° - 1600\,°C). \qquad (13)$$

Both ΔH_p [8, 25, 33] and ΔH_i [8, 25, 34, 35] are best given as about 1.0 eV for ThO_2 containing 10 – 20 mole % $YO_{1.5}$ (ΔH_i increases to 1.1 eV at 25 mole % $YO_{1.5}$ [8] and to 1.2 eV at 29 mole % $YO_{1.5}$ [29]).

The $P_{\oplus}$ value qualitatively agrees with emf measurements at intermediate oxygen pressures which are generally reported as slightly low when P'_{O_2} is established with a Cu – Cu_2O electrode ($t_i = 0.99$ at 1000 °C), but often found to be quite accurate with a Ni – NiO electrode ($t_i = 0.999$ at 1000 °C) [1]. For $P'_{O_2} = 10^{-18}$ atm, $\bar{t}_i \geqq 0.99$ for $P''_{O_2} \leqq 10^{-2}$ atm following Eq. (3), (4), (6), and (7).

Low Oxygen Pressures

Table 3 summarizes the experimental investigations of $P_{\ominus}$ for ThO_2-based solutions which have

Table 3. Log $P_{\ominus}$ values for ThO_2-based electrolytes.

Addition to ThO_2 [mole %]	Sample Shape	Purity	Technique	Temperature Range [°C]	log $P_{\ominus}$ [atm] 1000 °C	Ref.
10% $YO_{1.5}$	disk	99.997	Emf comparison, Mn-MnO vs. Fe-Fe_xO, Nb-NbO vs. Fe-Fe_xO	800–1050	– 33[a]	8
15% $YO_{1.5}$	disk	99.82	D-c polarization, Au vs. Nb-NbO	800–1000	– 42	26
15% $YO_{1.5}$	tube[b]	99.87	Coulometric titration, O_2 out of air	727–1127	– 32	36
14% $YO_{1.5}$	disk	99.9	Emf comparison, Ta-Ta_2O_5 vs. Fe-Fe_xO	700–1100	– 29[c]	37
15% $YO_{1.5}$	disk	99.6	Maximum emf, Th-ThO_2 vs. NbO-NbO_2	775–1000	– 30	38
29% $YO_{1.5}$	disk		Emf comparison, Si-SiO_2 vs. Ni-NiO	600–1000	– 13[d]	39
15% $YO_{1.5}$	disk		Emf comparison, Zr-ZrO_2 vs. Nb-NbO	927–1175	– 33	35

[a] Estimated. [b] In series with a ZrO_2+15% CaO tube. [c] 1027 °C. [d] Reported as an apparent value.

been reported. In one instance [35], using the reported E_m value, $P_\ominus$ was calculated from Eq. (2) for $P_\ominus \gg P''_{O_2}$.

The trend in Table 3 is strikingly comparable to that both in Table 1 and the results of an earlier study [2], i. e., the emf comparison and maximum emf results are usually higher than those from coulometric titration and the d – c data are unreliable.

The very high apparent $P_\ominus$ value in Table 3 derived from the emf comparison technique [39], which has always led to values which are too high for stabilized zirconia electrolytes [2], provides further strong evidence of the experimental difficulties generally associated with emf measurements in regions of appreciable electronic conduction in the electrolyte and always associated with emf measurements at low oxygen potentials. In particular, polarization of the anode through oxidation by the gas phase or by oxygen which is unavoidably transferred through the electrolyte lowers the measured emf and, in turn, raises the apparent $P_\ominus$. A further danger is that emf reproducibility upon changing the temperature, gas flow rate, cell configuration, and reference electrode [39] is no guarantee of the absence of electrode polarization (or other deleterious effects such as electrode-electrolyte or electrode-gas chemical interactions).

Unfortunately, use of two electrolyte pellets with an electronically conducting barrier between them [39] should generally not be expected to alleviate the problem of open-circuit oxygen transfer. If the barrier did not allow oxygen ions to be supplied or consumed and did lower oxygen transfer, it would have an oxygen chemical potential gradient across it and thereby lower the cell emf. If it were porous or fit poorly between the electrolytes enabling the gas phase to establish the same oxygen pressure, $P^b_{O_2}$, at both barrier-electrolyte interfaces, then for $P^b_{O_2} > P''_{O_2}$, an even greater oxygen flux to the anode would be expected. Some improvement could be realized with a reversible electrode as the barrier if $P''_{O_2} > P^b_{O_2} > P'_{O_2}$.

Electrolyte porosity must obviously be avoided and can be especially detrimental to emf measurements. At least partly on this account, significant deviations from the theoretical emf's for the cell

$$H_2 - H_2O/Th_{0.85}Y_{0.15}O_{1.925}/air$$

were observed at anode oxygen pressures of only 10^{-18} and $10^{-8.5}$ atm at 1000° and 1600 °C, respectively [40]. Higher $H_2 - H_2O$ flow rates will somewhat improve cell behaviour by lowering anode polarization [2].

As a consequence of oxygen transfer from cathode to anode and possible influence from the gaseous environment, high $P_\ominus$ values from other studies involving the emf comparison and maximum emf techniques must be suspected. Nonetheless, general consistency among the emf results and their agreement with coulometric titration data are notably better for thoria-based than stabilized zirconia electrolytes [2], partly due to their lower conductivities which reduces oxygen transfer. In addition, two-phase solid or liquid electrodes with high ionic and atomic diffusion coefficients can be less polarizable than Pt, $H_2 - H_2O$ or Pt, $CO - CO_2$ electrodes which have been used in several stabilized zirconia investigations. The recent low emf value [35] in Table 3 may indicate the advantage in keeping the oxygen activity gradient across the electrolyte low. Lastly, one of the higher values [38] could, at least in part, be attributed to the relatively impure samples. Easily reducible impurities facilitate oxygen loss from the electrolyte by accepting electrons and then may act as electron donors to increase n-type conductivity. They will be particularly influential in ThO_2-based solutions since n-type conductivity is extremely low.

The coulometric titration technique has been concluded to be the most reliable [2]. Relatively simple experimentally, it offers the best reproducibility as well as the best consistency with independent thermodynamic property determinations using similar electrolytes. In effect, unwanted oxidation of the anode is overcome by preliminary electrochemical reduction of oxygen at the anode-electrolyte interface. However, after removing the external voltage, the cell emf must be recorded rapidly * before oxygen diffusion in the anode compartment and oxygen migration through the electrolyte destroy the necessary condition that $P'_{O_2} \ll P_\ominus$. At the required very low P'_{O_2} values, the buffering capacity of the anode will be very low meaning that only small oxygen additions will greatly increase the oxygen activity.

One should recognize that it is extremely difficult, if not impossible, to attain a very low oxygen activity in the anode compartment itself. When electrolyte disks are used, high-temperature seals are required to isolate the electrode chambers. Elimina-

* A high-resistance potentiometer should be used to minimize re-oxidation of the anode.

tion of this problem by the use of impervious electrolyte tubes introduces the problem of oxygen transfer in the hot zone through the sides of the electrolyte.

Open-circuit oxygen transfer can be quantitatively described by applying WAGNER's theory of tarnishing reactions [41] to oxides with fully ionized defects which gives

$$i_i = -i_e = \frac{1}{4F} t_i t_e \sigma_t \frac{d\mu_{O_2}}{dx} \qquad (14)$$

where i_i and i_e are the ionic and electronic current densities through the oxide, t_i and t_e are the ionic and electronic transport numbers, μ is chemical potential, and x is the distance across the oxide measured from the low oxygen-pressure side. Substituting $\sigma_i = t_i \sigma_t$ and integrating leads to

$$i_i = -i_e = \frac{RT}{4Fl} \sigma_i \int_{P_{O_2}'}^{P_{O_2}''} t_e \, d \ln P_{O_2} \qquad (15)$$

where l is the thickness of the oxide. Since $t_e = 1 - t_i$ and t_i is given by Eq. (4), Eq. (15) can be evaluated. For $P_\oplus \gg P_{O_2}'' \gg P_\ominus$,

$$i_i = \frac{RT}{Fl} \sigma_i \ln \frac{P_\ominus^{1/4} + P_{O_2}'^{1/4}}{P_{O_2}'^{1/4}} \qquad (16)$$

or, by comparison with Eq. (2) and (3),

$$i_i = (\sigma_i/l)(E_t - E_m). \qquad (17)$$

Under this condition, it is evident that oxygen permeability is unaffected by the oxygen pressure at the reference electrode (P_{O_2}'').

Liquid metals containing dissolved oxygen have been used as anodes for the coulometric titration technique [2]. Consider the cell

$$(-)\ O(\text{in Cu})/ThO_2 - Y_2O_3/Co - CoO\ (+)$$

whereby a $ThO_2 - Y_2O_3$ tube is immersed in liquid copper. Applying an external voltage such that the copper electrode becomes the cathode causes deoxidation of the liquid metal. The rate of oxygen removal, controlled by diffusion and convection in the metal, cannot exceed a limiting current density i_l, which can be realized for small depths of immersion of the electrolyte tube [42]. Simultaneously, due to electronic conductivity in the electrolyte, oxygen will enter the liquid metal compartment through that part of the tube above the electrodes.

Taking 1200 °C as an example, for gently stirred copper, the effective or Nernst diffusion layer thickness is about 0.04 cm from which i_l can be calculated [42]. For 1.55×10^{-5} atomic % oxygen in copper (equivalent to $P_{O_2} = 10^{-15}$ atm), $i_l = 9 \times 10^{-3}$ mA/cm². From Equation (16), the opposing ionic current into the liquid metal side of the cell can be determined. In the $ThO_2 - Y_2O_3$ system, the maximum conductivity appears at about 14 mole % $YO_{1.5}$ [8, 9] for which, based on the available conductivity data [1],

$$\sigma_i = 92.4 \exp(-23{,}100/RT). \qquad (18)$$

(This equation was used to plot σ_i in Figure 1.) Using $T = 1473$ °K, $l = 0.2$ cm, $\sigma_i = 3.4 \times 10^{-2}\ \Omega^{-1}$ cm^{-1}, $P_\ominus = 10^{-27}$ atm (see Fig. 2), and $P_{O_2}' = 10^{-15}$ atm in Eq. (16) gives $i_i = 2 \times 10^{-2}$ mA/cm². Theoretically, therefore, for equal areas of the liquid metal-electrolyte interface and the remaining part of the electrolyte tube in the hot zone, the oxygen potential in the liquid metal compartment cannot even be lowered to 10^{-15} atm since the permeation rate exceeds the external current. Although lower activities could be realized in practice since the gas above the liquid metal will generally not remain in equilibrium with the metal during deoxidation, but exert a higher oxygen activity (which will decrease i_i or even reverse its direction depending upon the reference electrode), this calculation illustrates the potential seriousness of open-circuit oxygen transfer.

Furthermore, Eq. (16) gives the initial rate of oxygen return through the electrolyte to the anode-electrolyte interface after the external voltage is interrupted, e. g., $i_i = 25.3$ mA/cm² at 1000 °C for $P_{O_2}' = 10^{-8} P_\ominus$ (P_{O_2}' is defined by the external voltage). This will be complimented by i_l – the initial rate of oxygen diffusion from the bulk of the anode to the anode-electrolyte interface.

Consequently, it is not a priori certain in the coulometric titration technique that the subsequent emf measurement will satisfy the required condition that $P_{O_2}' \ll P_\ominus$. Increasing the applied voltage to further lower P_{O_2}' is unwise since electrolysis or even severe reduction of the electrolyte could destroy its bulk properties. Improvement is better accomplished by minimizing oxygen permeation through the electrolyte, i. e., by increasing l or decreasing P_{O_2}'' so that $P_{O_2}'' \sim P_\ominus$ [the latter necessitates use of the second term on the right hand side of Eq. (2) for E_m in Eq. (17) and slight adjustment of Eq. (8)].

Other techniques such as a-c conductivity, oxygen permeability, or diffusion coefficient measurements

are experimentally very difficult and would not be expected to yield accurate transport numbers.

From the available coulometric titration results [36],

$$\log P_{\ominus} = -\frac{57.9\times10^3}{T} + 13.4 \quad (700^\circ - 1100\,^\circ\mathrm{C})\ *. \tag{19}$$

Following Eq. (10), extrapolation to higher temperatures is only justified if ΔH_i and ΔH_n do not change. At first glance, it would appear, since emf measurements at $1500^\circ - 1600\,^\circ$C and 10^{-14} to 10^{-17} atm of oxygen [27, 43–45] indicate somewhat lower $P_{\ominus}$ values than predicted by Eq. (19), that either ΔH_i increases or ΔH_n decreases above 1100 °C. The former seems more likely but possible reasons for slope changes in Arrhenius plots of ionic conductivity [46] such as defect association between yttrium ions and oxygen vacancies and irregular lattice parameter changes have resulted in lower activation energies at the higher temperatures in the case of $ZrO_2 - Y_2O_3$ [47, 48] and $ZrO_2 - CeO_2 - Y_2O_3$ [46] electrolytes, respectively. Grain boundary conduction in oxides is usually negligible [1] and no evidence of an order-disorder transformation in ThO_2-based electrolytes has yet been advanced **, although some degree of order on the anion sublattice is expected [49]. In any case, it is quite probable that any order-disorder changes will not affect ΔH_i [1]. Also, from the conductivity results of WIMMER, BIDWELL, and TALLAN [25], an increase in ΔH_i at high temperatures does not appear to be the case. Possible changes in ΔH_n remain to be seen, but a decrease at high temperatures is improbable.

SHORES and RAPP [50] have recently shown that, because TRET'YAKOV and MUAN [36] used a bielectrolyte cell, their $P_{\ominus}$ values could be about one order of magnitude lower than those given by Eq. (19) if the oxygen pressure at the interface between the $ZrO_2 - CaO$ and $ThO_2 - Y_2O_3$ electrolytes was dictated by the rates of ionic and electronic transport through the cell. Such a change leads to improved consistency with the aforementioned high-temperature emf studies.

Accordingly, based on the preceding arguments, $P_{\ominus}$ for $ThO_2 - Y_2O_3$ solutions is best given as

$$\log P_{\ominus} = -\frac{57.9\times10^3}{T} + 12.4 \quad (700^\circ - 1600\,^\circ\mathrm{C}). \tag{20}$$

Comparison of Eq. (10) and (20) yields $\Delta H_n = 3.9$ eV in close agreement with a recently quoted value of 4.1 eV [38].

At low temperatures, Eq. (20) concurs semi-quantitatively with thermodynamic studies at low oxygen potentials involving ThO_2-based electrolytes that have indicated, based on observations of stable, reproducible emf readings in good accord with expected values, that t_e is very low down to 10^{-24} to 10^{-25} atm of oxygen at 1000 °C [1]. From Eq. (20) and (4), $t_i = 0.99$ for these conditions. Furthermore, in the cell

$$Nb - NbO/ThO_2 - Y_2O_3/Fe - Fe_xO$$

for which $P'_{O_2} = 10^{-25}$ atm [51, 52] and $P''_{O_2} = 10^{-15}$ atm [53] at 1000 °C, $\bar{t}_i = 0.998$ according to Eq. (20), (2), (3), and (7) ($P_{\ominus} \gg P''_{O_2}$). From Eq. (20), it appears that a thermodynamic investigation using the cell

$$Pr - Pr_2O_3/Th_{0.82}Y_{0.18}O_{1.91}/Fe - Fe_xO$$

at $800^\circ - 1000\,^\circ$C [54] was unwittingly a $P_{\ominus}$ determination via the maximum emf method since $P'_{O_2} = 10^{-33.3}$ atm at 1000 °C was reported.

Agreement at 1600 °C comes from WIMMER, BIDWELL, and TALLAN [25] who show the p-n transition at $P_{O_2} = 10^{-8}$ atm. As $P_{\ominus} = 10^2$ atm, one would predict $P_{\ominus} = 10^{-18}$ atm assuming $\sigma_n \propto P_{O_2}^{-1/4}$. However, indirectly, from successful emf measurements on the cell

$$Si - SiO_2/Th_{0.85}Y_{0.15}O_{1.925}/Cr - Cr_2O_3$$

at 1500° and 1600 °C, FRUEHAN [44] has implied still greater stability for $ThO_2 - Y_2O_3$ electrolytes than given by Equation (20). At 1600 °C, $P'_{O_2} = 10^{-16}$ atm and $P''_{O_2} = 10^{-12}$ atm [55] for this cell. Satisfactory behaviour under these conditions has been verified in a recent study of $Fe - Al - O$ alloys [45]. Taking $\bar{t}_i = 0.98$ as a lower limit yields $P_{\ominus} = 10^{-21}$ atm at 1600 °C. Very pure electrolytes, even ones devoid of easily reducible cations, can lower $P_{\ominus}$ values by $2 - 3$ orders of magnitude [2], but the purity of Fruehan's electrolytes was not stated. It is felt that Eq. (20) will apply reasonably well to most commercially-available materials.

The $P_{\ominus}$ values for ThO_2-based solutions are $3 - 5$ orders lower than those for stabilized zirconia [2], in qualitative agreement with the greater thermodyna-

* This equation has been recalculated from the E_{max} data given by Tret'yakov and Muan using Eq. (8) and differs somewhat from theirs.

** For example, in $ThO_2 - Y_2O_3$ electrolytes, anion vacancies may preferentially coordinate with the smaller Y^{3+} cations at low temperatures.

mic stability of ThO_2. Oxygen pressures about four orders lower for ThO_2 than tetragonal ZrO_2 have been reported to produce similar oxygen deficiencies at $1400° - 1900\,°C$ [22] and decomposition pressures for ThO_2 are $4 - 8$ orders lower between $700°$ and $1600\,°C$ [55]. However, comparison of decomposition pressures, $P^d_{O_2}$, to quantitatively define $P_\ominus$ [56] is unwarranted since this presupposes similar excess electron concentrations at a given $P_{O_2}/P^d_{O_2}$ and similar electron mobilities, and neglects the facts that stabilized ZrO_2 has a different structure than ZrO_2 and ionic conductivities for the two systems differ by more than an order of magnitude [1].

Summary and Conclusions

Equations (9), (11), (13), and (20) and high-temperature results for ThO_2 [12, 13] have been plotted in Figure 2. The solid lines can be regarded as fairly well established, whereas the dashed lines for ThO_2 are tentative and await confirmation or refinement. Nevertheless, more data for ThO_2-based solutions above $1200\,°C$ at low oxygen potentials are highly desirable.

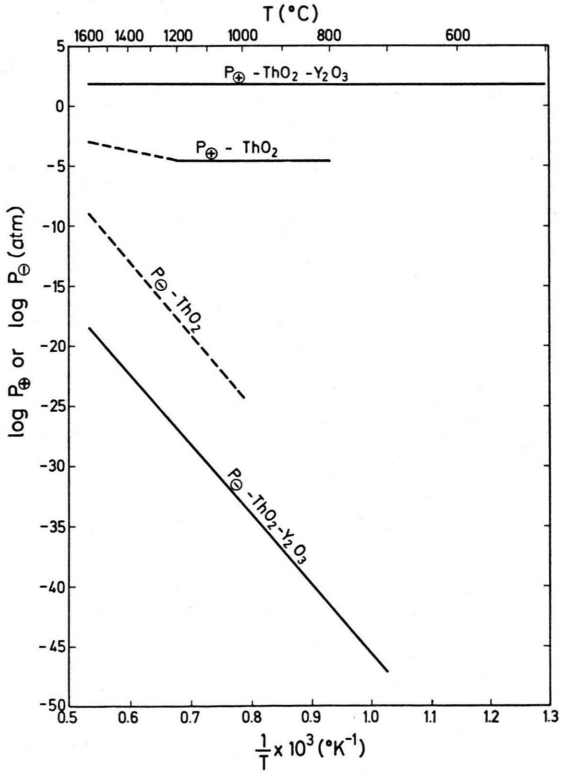

Fig. 2. The parameters $P_\oplus$ and $P_\ominus$ for ThO_2 and ThO_2–Y_2O_3.

Although transport numbers will unavoidably vary somewhat among different oxide samples, ideal behaviour for reasonably pure materials can certainly only be assumed if they do not differ significantly from those which can be calculated from Figure 2. Use of very pure materials for ThO_2-based solutions could lower $P_\ominus$ by $2 - 3$ orders of magnitude.

Average ionic transport numbers, calculated from Eq. (2), (3), and (7), in cells with ThO_2-based electrolytes for five possible reference electrodes are plotted against the oxygen potential at the other electrode in Fig. 3 and 4 for temperatures of 1000°

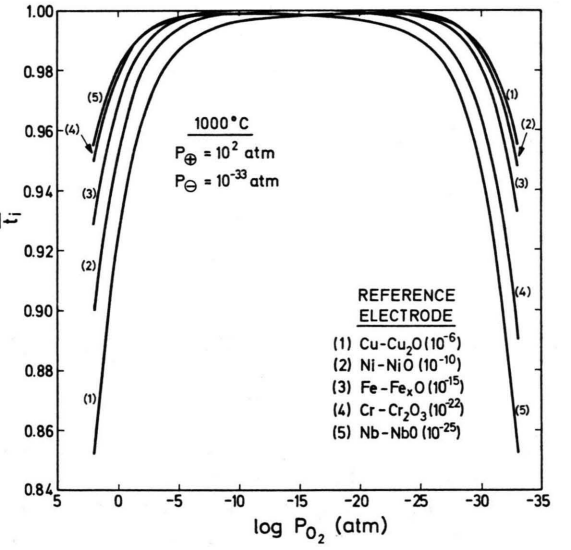

Fig. 3. Average ionic transport numbers for cells with ThO_2-based solid electrolytes at 1000 °C. The equilibrium oxygen potentials imposed by the reference electrodes are shown in brackets.

and 1600 °C, respectively. Thermodynamic data for the reference electrodes were taken from the following sources: $Cu - Cu_2O$ [53, 57] (OSTERWALD's data [57] were extrapolated from 1300 °C), $Ni - NiO$ and $Fe - Fe_xO$ [53, 55] (neglecting mutual solubility of the phases at 1600 °C), $Cr - Cr_2O_3$ [55, 58], and $Nb - NbO$ [51, 52] (extrapolated from 1100 °C).

Regarding t_i, it serves as a ready indication of the expected emf if a cell is functioning properly, i. e., interference from electrode polarization, electrolyte porosity, the gas phase, interdiffusion of electrode and electrolyte, and chemical reactions is absent. When $t_i = 1$ is assumed, it also defines the limits for the oxygen activity at the test electrode to keep the measurements within a permissible ac-

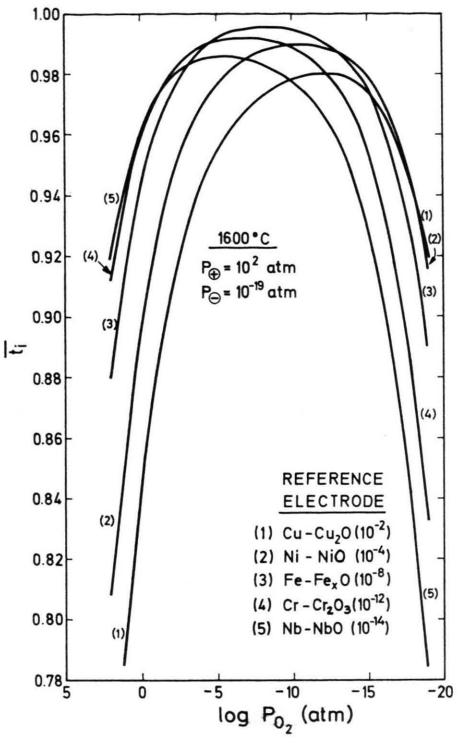

Fig. 4. Average ionic transport numbers for cells with ThO_2-based solid electrolytes at 1600 °C. The equilibrium oxygen potentials imposed by the reference electrodes are shown in brackets.

curacy for a given reference electrode, but, as recently pointed out [38], can be misleading if compared with respect to obtainable accuracy for different reference electrodes. For example, from Fig. 3 and 4, at high oxygen pressures $\bar{t}_i$ increases as the oxygen potential of the reference electrode, P'_{O_2} in this case, decreases (providing $P'_{O_2} \gg P_{\ominus}$) indicating, at first glance, improved cell behaviour. However, the error in calculating P''_{O_2} using Eq. (3) for E_m, i. e., assuming $t_i = 1$, is determined by $\Delta E = E_t - E_m = (1 - \bar{t}_i) E_t$ and not $\bar{t}_i$. From Equation (2) and Equation (6), ΔE actually increases as P'_{O_2} is lowered until $P'_{O_2} \ll P_{\ominus}$ at which point it becomes constant. Working in regions where t_i is not approximately unity and then attempting to correct the measured emf using $\bar{t}_i$ is a risky procedure on account of uncertain variations in transport numbers from electrolyte to electrolyte and possible interference from open-circuit oxygen transfer.

To cover a wide range of oxygen activities, $Fe - Fe_xO$ is the best reference electrode although it has, on occasion, been reported to react with $ThO_2 - Y_2O_3$ electrolytes [9, 51], apparently due to reaction between Fe_xO and Y_2O_3 [51] ($Co - CoO$ and $Mo - MoO_2$ provide alternatives). Nevertheless, for any given application, the oxygen potentials of the electrodes should be as close as possible to maximize the attainable accuracy (low E_t) and minimize oxygen transfer through the electrolyte. Under no conditions can $\bar{t}_i > 0.996$ be achieved at 1600 °C.

To determine transport numbers in oxides, a – c conductivity measurements or emf methods are best at high oxygen activities, whereas the coulometric titration technique and, occasionally, emf methods are superior at low oxygen activities.

At 700° – 1600 °C, although $P_{\ominus}$ for stabilized zirconia solutions [23] is approximately 10 – 16 orders of magnitude higher than for thoria-based solutions, $P_{\ominus}$ for the latter is 3 – 5 orders lower. However, the principal advantage of thoria-based solutions as solid electrolytes, their extreme stability at low oxygen potentials, can be quickly lost by the use of impure or porous electrolytes, injudicious choice of the reference electrode, or inadequate precautions to ensure that the bulk properties of the electrodes will be realized.

Acknowledgments

I wish to express my appreciation to Professor A. KLEMM for his hospitality during my stay in Mainz. Financial support was provided by the National Research Council of Canada.

[1] T. H. ETSELL and S. N. FLENGAS, Chem. Rev. **70**, 339 [1970].
[2] T. H. ETSELL and S. N. FLENGAS, J. Electrochem. Soc. **119**, 1 [1972].
[3] H. SCHMALZRIED, Z. Phys. Chem. N.F. **38**, 87 [1963].
[4] W. E. DANFORTH and F. H. MORGAN, Phys. Rev. **79**, 142 [1950].
[5] W. E. DANFORTH, Phys. Rev. **86**, 416 [1952].
[6] W. E. DANFORTH and J. H. BODINE, J. Franklin Inst. **260**, 467 [1955].
[7] S. F. PAL'GUEV and A. D. NEUIMIN, in: Electrochemistry of Molten and Solid Electrolytes, Vol. 1, Consultants Bureau, New York 1961, p. 90.
[8] B. C. H. STEELE and C. B. ALCOCK, Trans. Met. Soc. AIME **233**, 1359 [1965].
[9] M. F. LASKER and R. A. RAPP, Z. Phys. Chem. N.F. **49**, 198 [1966].
[10] E. C. SUBBARAO, P. H. SUTTER, and J. HRIZO, J. Amer. Ceram. Soc. **48**, 443 [1965].
[11] J. E. BAUERLE, J. Chem. Phys. **45**, 4162 [1966].
[12] I. BRANSKY and N. M. TALLAN, J. Amer. Ceram. Soc. **53**, 625 [1970]. – N. M. TALLAN and I. BRANSKY, J. Electrochem. Soc. **118**, 345 [1971].
[13] A. HAMMOU, C. DEPORTES, and G. ROBERT, J. Chim. Phys. **68**, 1162 [1971].
[14] J. RUDOLPH, Z. Naturforsch. **14 a**, 727 [1959].

[15] V. N. Chebotin, Z. S. Volchenkova, and S. F. Pal'guev, in: Electrochemistry of Molten and Solid Electrolytes, Vol. 4, A. N. Baraboshkin and S. F. Pal'guev, ed., Consultants Bureau, New York 1967, p. 123.

[16] J. L. Bates, U.S. At. Energy Comm. BNWL-457, 1967, 16 pp.

[17] R. C. Linares, J. Phys. Chem. Solids **28**, 1285 [1967].

[18] H. S. Edwards, A. F. Rosenberg, and J. T. Bittel, NASA Document N 63-20007, 1963, 146 pp.

[19] R. J. Hawkins and C. B. Alcock, J. Nucl. Mater. **26**, 112 [1968].

[20] A. D. King, J. Nucl. Mater. **38**, 347 [1971].

[21] T. H. Etsell and S. N. Flengas, J. Electrochem. Soc. **116**, 771 [1969].

[22] S. C. Carniglia, S. D. Brown, and T. F. Schroeder, J. Amer. Ceram. Soc. **54**, 13 [1971].

[23] L. Heyne and N. M. Beekmans, Proc. Brit. Ceram. Soc. **19**, 229 [1971].

[24] R. Benz, J. Nucl. Mater. **29**, 43 [1969].

[25] J. M. Wimmer,, L. R. Bidwell, and N. M. Tallan, J. Amer. Ceram. Soc. **50**, 198 [1967].

[26] J. W. Patterson, E. C. Bogren, and R. A. Rapp, J. Electrochem. Soc. **114**, 752 [1967].

[27] K. Schwerdtfeger, Trans. Met. Soc. AIME **239**, 1276 [1967].

[28] H. Ullmann, Z. Phys. Chem. **237**, 274 [1968].

[29] F. J. Salzano, C. Auerbach, H. S. Isaacs, and B. Minushkin, J. Electrochem. Soc. **118**, 416 [1971].

[30] M. Iqbal and E. H. Baker, Proc. Brit. Ceram. Soc. **19**, 279 [1971].

[31] L. D. Burke, H. Rickert, and R. Steiner, Z. Phys. Chem. N.F. **74**, 146 [1971].

[32] C. E. McGinley and P. Hancock, J. Mater. Sci. **6**, 260 [1971].

[33] H. Ullmann, Z. Phys. Chem. **237**, 71 [1968].

[34] R. E. W. Casselton, Phys. Stat. Sol. (a) **3**, K 255 [1970].

[35] A. V. Ramana Rao and V. B. Tare, Scripta Met. **5**, 813 [1971].

[36] Yu. D. Tret'yakov and A. Muan, J. Electrochem. Soc. **116**, 331 [1969].

[37] S. R. Levine and M. Kolodney, J. Electrochem. Soc. **116**, 1420 [1969].

[38] J. B. Hardaway III, J. W. Patterson, D. R. Wilder, and J. D. Schieltz, J. Amer. Ceram. Soc. **54**, 94 [1971].

[39] F. J. Salzano, H. S. Isaacs, and B. Minushkin, J. Electrochem. Soc. **118**, 412 [1971].

[40] W. A. Fischer and D. Janke, Z. Phys. Chem. N.F. **69**, 11 [1970].

[41] C. Wagner, Z. Phys. Chem. **B 21**, 25 [1933].

[42] T. H. Etsell and S. N. Flengas, J. Electrochem. Soc. **119**, 198 [1972].

[43] R. J. Fruehan, L. J. Martonik, and E. T. Turkdogan, Trans. Met. Soc. AIME **245**, 1501 [1969].

[44] R. J. Fruehan, Met. Trans. **1**, 865 [1970].

[45] R. J. Fruehan, Met. Trans. **1**, 3403 [1970].

[46] C. Deportes, G. Robert, and M. Forestier, Electrochim. Acta **16**, 1003 [1971].

[47] J. E. Bauerle and J. Hrizo, J. Phys. Chem. Solids **30**, 565 [1969].

[48] R. E. W. Casselton, Phys. Stat. Sol. (a) **2**, 571 [1970].

[49] W. W. Barker and O. Knop, Proc. Brit. Ceram. Soc. **19**, 15 [1971].

[50] D. A. Shores and R. A. Rapp, J. Electrochem. Soc. **118**, 1107 [1971].

[51] W. L. Worrell, in: Thermodynamics, Vol. I, International Atomic Energy Agency, Vienna 1966, p. 131.

[52] G. B. Barbi, Z. Naturforsch. **23 a**, 800 [1968].

[53] G. G. Charette and S. N. Flengas, J. Electrochem. Soc. **115**, 796 [1968].

[54] U. Lott, H. Rickert, and C. Keller, J. Inorg. Nucl. Chem. **31**, 3427 [1969].

[55] O. Kubaschewski, E. Ll. Evans, and C. B. Alcock, Metallurgical Thermochemistry, 4th ed., Pergamon Press, London 1967.

[56] A. A. Vecher and D. V. Vecher, Russ. J. Phys. Chem. **42**, 418 [1968].

[57] J. Osterwald, Z. Phys. Chem. N.F. **49**, 138 [1966].

[58] Yu. D. Tret'yakov and H. Schmalzried, Ber. Bunsenges. Phys. Chem. **69**, 396 [1965].